

FATIGUE OF STEEL SPECIMENS AT LOW TEMPERATURES

ZAMOR ČELIČNIH UZORAKA PRI NISKIM TEMPERATURAMA

Alexander TESAR

ORIGINALNI NAUČNI RAD
ORIGINAL SCIENTIFIC PAPER
UDK:624.21.014.2
doi:10.5937/GRMK2003003T

1 INTRODUCTION

Fatigue behaviour of steel specimens at low temperatures has recently become the focus of intense efforts in structural engineering. This is because of pressing problems of fatigue disaster prevention in long-termed exploitation of steel specimens appearing in slender structures, such as space and offshore facilities, guyed masts, cable roofs, bridges or lines of high voltage air conductors located in northern territories and subjected to heavy dynamic loads under low temperatures. Sophisticated analysis is required in order to answer the questions associated with fatigue behaviour and reliability of such specimens.

Simulation models adopting the wave analysis on the micro-mechanical level was used for fatigue research considering the behaviour of multi-string elements configurated in backpropagation neural network. Such models have been developed and treated by Tesar, A. ([1], [2], [7], [11]), Simo, J.C. ([3]), Huston, R.I. and Passerello, C.E. ([4]), Adeli, H. and Yeh, C. ([5]), Lu, W. and Mäkeläinen, P. ([6]), Budiansky, B. ([8], [9]) and others.

This paper deals with:

1. mathematical formulation of governing wave equations for fatigue analysis of steel specimens at low temperatures,
2. brief description of ultimate fatigue analysis at low temperatures adopting the parallel processing FETM-wave approach with backpropagation neural network,
3. numerical and experimental analyses.

$$I = \int_V [S_{ij} \varepsilon_{ij} + 0.5 W_{ij} u_{ki} u_{kj} - (\varepsilon_{ij}^0 + 0.5 \varepsilon'_{ij}) S_{ij}] dV - \int_{A1} r_i^{(-)} u_i dA1 - \int_{A2} s_i (u_i - w_i) dA2 \} (dt)^2 + \int_V W_{ij} \varepsilon_{ij} dV - \int_{A1} r_i u_i dA1 - \int_{A2} p_i (u_i - w_i) dA2 \} dt \quad (1)$$

Alexander Tesar, Civ.Eng., PhD., DrSc., assoc.prof., FEng., authorized engineer of Slovak Chamber of Civil Engineers, Bratislava, Slovak Republic, alexander.tesar@gmail.com

2 FATIGUE BEHAVIOUR AT LOW TEMPERATURES

If a steel specimen consists of densely packed inclusions, the interaction effects of inclusions play a dominant role in fatigue behaviour of resulting continuum at low temperatures. The concept of transformation strain can be used when an elastic medium contains periodically distributed inclusions or voids in the material. Because of periodicity, the transformation strains as well as other field quantities entering into estimate of elastic moduli are periodic functions of space, time and temperature. The periodicity is exploited in an effort to obtain accurate estimates for transformation strains used to approximate mechanical properties of steel specimens at low temperatures.

The Washizu's variation principle is adopted below in order to include initial stress and strain components due to isothermal deformations in time. The stress in microelements of the model adopted at the beginning of time increment studied is considered as initial stress and thermal strain increment ([8], [9]). The variation principle under consideration is written in terms of time rate quantities given by

where W_{ij} and S_{ij} are the Piola-Kirchhoff stress tensors for initial stress and strain rate states, respectively, p_i and s_i are the Lagrange surface traction and its time rate quantity, respectively, r_i and $r_i^{(-)}$ are prescribed on surface

area A1, w_i on area A2 and V is the volume bounded by area $A=A1+A2$. The total strain rate ε_{ij} is composed of initial strain rates ε^{0ij} and ε'_{ij} , corresponding to instantaneous stress rate S_{ij} . To evaluate the strain rate, thermal expansion coefficient at temperature T be $\alpha(T)$ and at temperature $T+dT$ be $\alpha(T+dT)$ is adopted. By expanding $\alpha(T+dT)$ into Taylor series, the average thermal strain rate is obtained.

Governing wave equation for treatment of ultimate fatigue behaviour of elastic continuum at low temperatures ([10]) is given by

$$\mu \eta(u_t) + (\lambda + \mu) \text{grad}(\text{div } u_t) + f = \rho \partial^2 u_t / \partial t^2, \quad (2)$$

where λ and μ are Lamé constants, mass density is ρ , corresponding Laplace operator is η , the body force vector is f and the vector of displacements is u_t .

In terms of derivatives of displacement components u_t , the governing wave equation is modified as

$$c_2 u_t + (c_1^2 - c_2^2) u_t + f/\rho = a_t, \quad (3)$$

with propagation velocities for dilatational waves

$$c_1 = \sqrt{[(\lambda + 2\mu)/\rho]}, \quad (4)$$

and shear waves

$$c_2 = \sqrt{(\mu/\rho)}. \quad (5)$$

Strain and stress components are defined by

$$\varepsilon_{ij} = (u_{i,j} + u_{j,i})/2, \quad (6)$$

$$\sigma_{ij} = \lambda \varepsilon_{kk} \delta_{ij} + 2 \mu \varepsilon_{ij}, \quad i, j = 1, 2, 3, \quad (7)$$

with Kronecker delta function δ_{ij} .

3 PARALLEL PROCESSING

Mathematical and physical backgrounds of micromechanical simulation, based on the idea of parallel processing as part of backpropagation neural network approach ([11]), are described below.

The Euclidean n-dimensional space B^n is assumed. An open interval (a,b) is stated in B^1 , assuming $a < b$, $a, b \in B^1$ and $\langle a, b \rangle$ being contained in B^1 . The symbol $G^{(k)}(a,b)$, with $k \in \mathbb{N}$, is a set of real functions with continuous derivatives of the order s ($0 \leq s \leq k$) in (a,b) . $C^{(k)}(\langle a, b \rangle)$ is the set of functions from $C^{(k)}(a,b)$, with derivatives continuously expanded into $\langle a, b \rangle$. $L(B^n)$ is the set of real matrices $n \times n$.

Let in $\langle a, b \rangle$ be assumed the system of n-linear differential equations of first order, given by

$$u_i'(t) = \sum a_{ij}(t) u_j, \quad i = 1, 2, \dots, n, \quad (8)$$

where $a_{ij}(t) \in C^{(0)}(\langle a, b \rangle)$ holds for all i and j .

In vector notation the system (8) is given by

$$u' = A u. \quad (9)$$

Definition 1. An n-dimensional column vector $u(t) = [(u_i(t))_{i=1}^n]^T$ is solution of system (9) if

$$\forall j: u_j(t) \in G^{(1)}(\langle a, b \rangle), \quad (10)$$

$$\forall t \in \langle a, b \rangle: u' = A u. \quad (11)$$

Theorem 1. The treatment of system (9) creates the n-dimensional vector space in the field of real numbers. The matrix having n-columns and containing all fundamental solutions of system (9) is denoted by $\Phi(t)$.

Theorem 2. Necessary and sufficient condition for the validity of the matrix $\Phi(t)$ for solution $\{\Phi_i(t)\}_{i=1}^n$ of system (9) is $\det \Phi(t) \neq 0$, where G is constant regular matrix of the same type.

Definition 2. An $n \times n$ square matrix of type

$$U_A(a,t) = \Phi(t) \Phi^{-1}(a), \quad \forall t \in \langle a, b \rangle, \quad (12)$$

holds in the interval $\langle a, b \rangle$.

The simulation model for fatigue behaviour is established by micromechanical string made of spring elements as shown in Fig. 1.

For physical interpretation of above definitions the internal and left-hand external wave displacements of the spring element are denoted by u_a and u_b . The u_a will match the u_b when the microelement is moved one bay to the right, so that u_a and u_b share the same dimension.

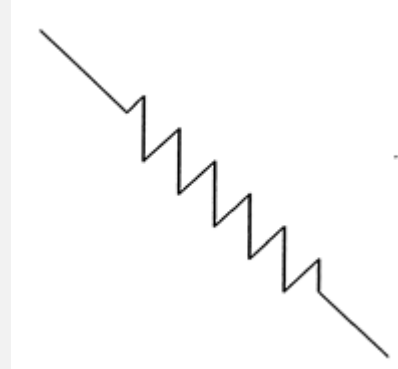


Fig. 1. Single spring microelement adopted

The internal wave displacement vector u_i is eliminated beforehand, giving the stiffness matrix

$$K(\omega) = \begin{bmatrix} K_{aa} & K_{ab} \\ K_{ba} & K_{bb} \end{bmatrix} \quad (13)$$

and displacement wave vector by

$$u = \begin{bmatrix} u_a \\ u_b \end{bmatrix}. \quad (14)$$

Corresponding force wave vectors are given by

$$n_a = K_{aa} u_a + K_{ab} u_b, \quad (15)$$

$$n_b = -K_{ba} u_a - K_{bb} u_b. \quad (16)$$

State wave vector v is defined as combination of wave displacements and forces given by

$$v = [u, n]^T. \quad (17)$$

Wave state vector at boundaries a and b is given by

$$v_b = S v_a, \quad (18)$$

adopting corresponding wave transfer matrix S . It holds

$$S = \begin{bmatrix} S_{aa} & S_{ab} \\ S_{ba} & S_{bb} \end{bmatrix}, \quad (19)$$

with

$$\begin{aligned} S_{aa} &= -K_{ab}^{-1} K_{aa} \quad , \quad S_{ab} = K_{ab}^{-1} \quad , \\ S_{ba} &= -K_{ba} + K_{bb} K_{ab}^{-1} K_{aa} \quad , \quad S_{bb} = -K_{bb} K_{ab}^{-1} \quad . \end{aligned} \quad (20)$$

The damping parameters are contained in the complex elasticity moduli appearing in the stiffness terms of corresponding transfer matrix S.

The calculation run of the FETM-wave approach which is adopted below with updated variability of the mesh size in space, time and temperature. The details of parallel processing FETM-wave approach are summed up, for example, in [1], [2], [3] or [4].

4 NEURAL NETWORK

Neural network has been developed for solution of some sophisticated problems in structural engineering. Compared to conventional digital computing techniques, neural networks are advantageous because of their special features, such as parallel processing, distributed storing information, low sensitivity of error, robustness in operation after training and adaptability to new information.

The idea for application of the neural network in structural engineering appeared in [5]. Neural networks have been used in structural analysis and design, material behaviour and damage identification.

Among such applications the neural network trained by backpropagation algorithm appears as most utilized neural network today, primarily due to its simplicity.

The topology of backpropagation neural network and training algorithm adopted [6] are described briefly below. It is a multilayered feed forward neural network trained by backpropagation algorithm.

The topology of neural network is plotted in Fig. 2, including the input layer, one or several hidden layers and the output layer. The fundamental building block of neural network called artificial node is shown in Fig. 3.

The node is composed of connecting springs, an adder using to sum the weighted input, an activation

function used to decrease the magnitude of the output and a threshold for activation function.

The backpropagation algorithm starts with randomly initialised weights. Using the calculation rule for one node, the input vector is feed-forwarded from layer to layer until the output is produced.

5 FATIGUE ANALYSIS

It is in nature of things that fatigue cracks are initiated as a result of cumulative ultimate damage process in structure.

As with any other ultimate state, the assessment of fatigue is carried out in demonstrating that strength function is higher compared with relevant ultimate fatigue resistance of the steel specimen studied at low temperatures.

The calculation rule for one basic node of the backpropagation neural network is given by

$$y = f(\text{net}) = f(\sum w_i x_i - \Theta) \quad , \quad (21)$$

where x_i is i-th component of input vector, w_i is i-th component of weight vector, Θ is threshold adopted, f is activation function, y is output of the node and t_i is i-th component of target vector, which is the desired output of neural network corresponding to input vector.

The backpropagation algorithm starts with randomly initialised values. Using the calculation rule for one node the input vector is feed-forwarded from layer to layer until the output is produced. The output vector is compared with target vector and the error in the output layer is calculated using

$$\delta_{pk} = (t_{pk} - o_{pk}) f_k (1 - f_k) \quad , \quad (22)$$

where t_{pk} and o_{pk} represent target and output values of the k-th node in the output layer corresponding to the p-th training pattern and f_k is the activation function for the k-th node.

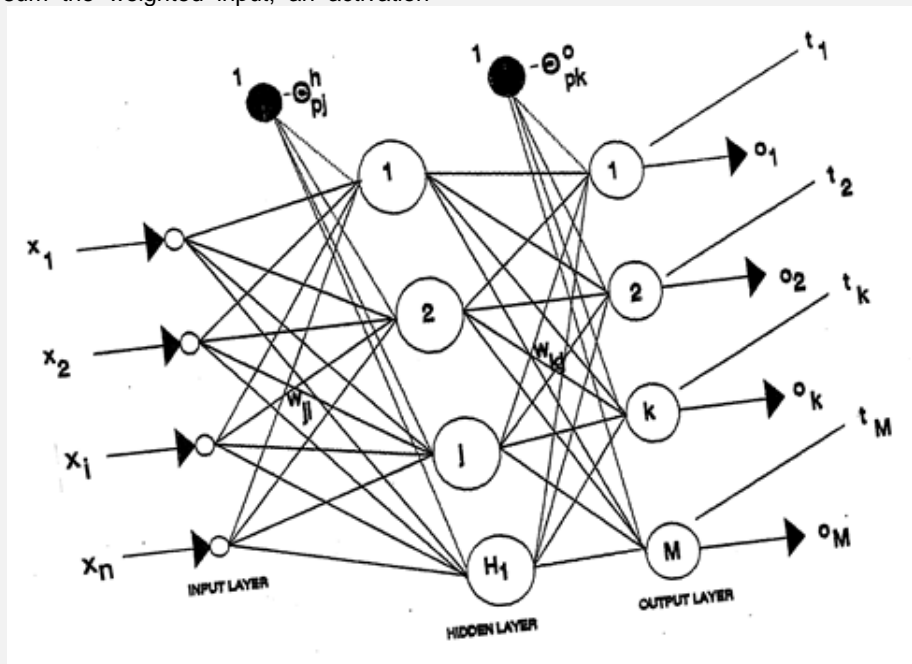


Fig. 2. Topology of the backpropagation neural network adopted

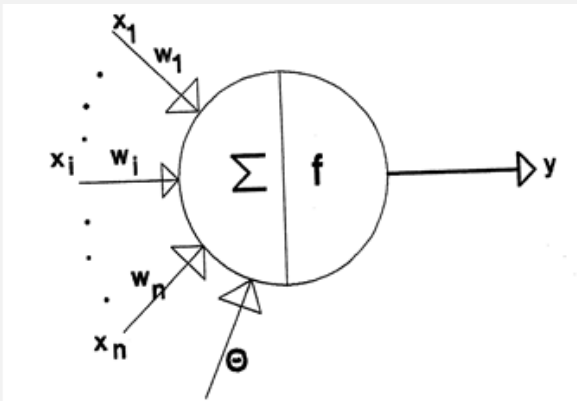


Fig. 3. Artificial node

Adopting the approach, calculation of ultimate fatigue analysis ([1], [10]) is given by:

Micromechanical modelling of material and structural configurations of specimen in space, time and temperature.

Updated calculation of wave stress and strain states in space, time and temperature as well as low and high cyclic structural response in each step of forcing and deformation process being stated in all microelements of the model adopted.

Comparison with ultimate fatigue strength stated in the Wöhler curve for the steel material used.

Initiation of cracks in micro-mechanical elements trespassing the ultimate fatigue strength in corresponding Wöhler curve,

Updated calculation of fatigue crack growth with the development of cracks in space, time and temperature, until fatigue destruction of the specimen is studied.

The regime of crack initiation and growth is rather complex. One or several cracks develop and propagate slowly along critical regions of the specimen studied. In the case of shear loading the cracks turn inside the body in a direction that is quasi-perpendicular to the tension ([3], [4], [5], [6] or [7]).

6 APPLICATION

Above approaches were adopted for numerical and experimental research of fatigue behaviour of steel specimen as shown in Fig. 4, subjected to static and dynamic loads at low temperatures.

Calculation mesh was adopted as well as stress-strain curve of specimen which is plotted in Figs. 5 and 6, respectively.

In numerical/experimental assessment static and dynamic tests at low temperatures were made. The pulsator with loading capacity of 6000 kN was adopted for experimental research, and it was established at the Institute of Construction and Architecture of Slovak Academy of Sciences in Bratislava, Slovak Republic (Fig. 7).



Fig. 4. Steel specimen studied

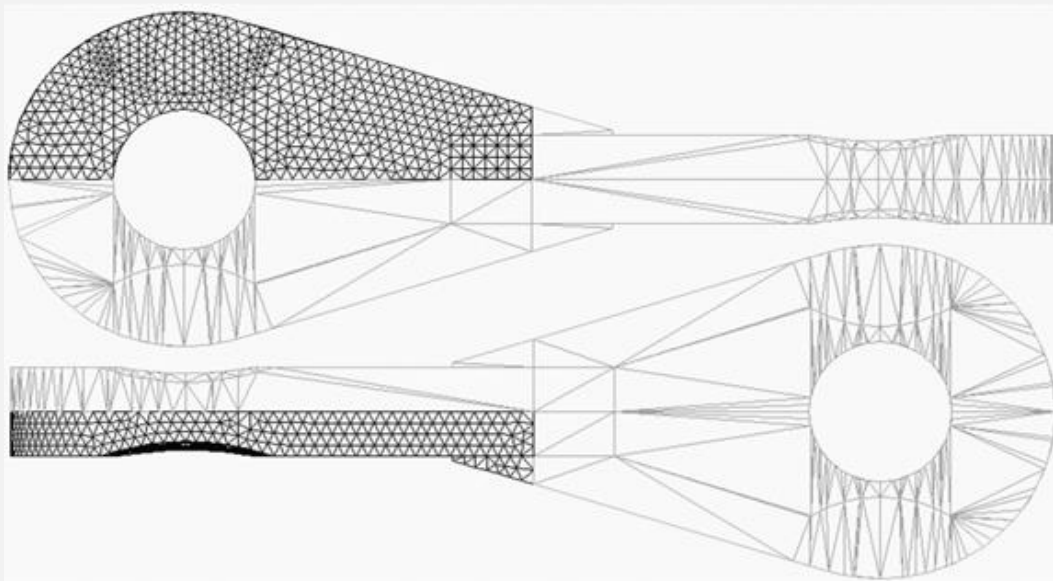


Fig. 5. Calculation mesh adopted

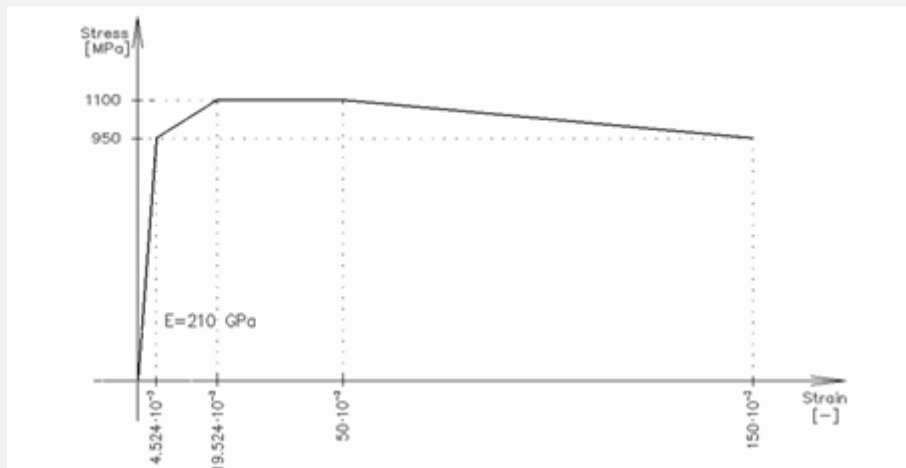


Fig. 6. Stress-strain curve of the specimen studied

The low temperatures were obtained in special insulated tube filled with dry ice where seven specimens were located in scope of experimental research (Fig. 8). Specimens were tested at temperature values in scope from -60°C until $+25^{\circ}$ and simultaneously were subjected to axial loads being updated until fatigue collapse.

The flow-chart of static testing:

Updated increase of axial static loading until the level 450 kN, with following decrease on the level 79 kN (the laboratory weight of testing platform).

Updated increase of axial static loading until the collapse of the studied specimen.



Fig. 7. Pulsator with loading capacity of 6000 kN adopted

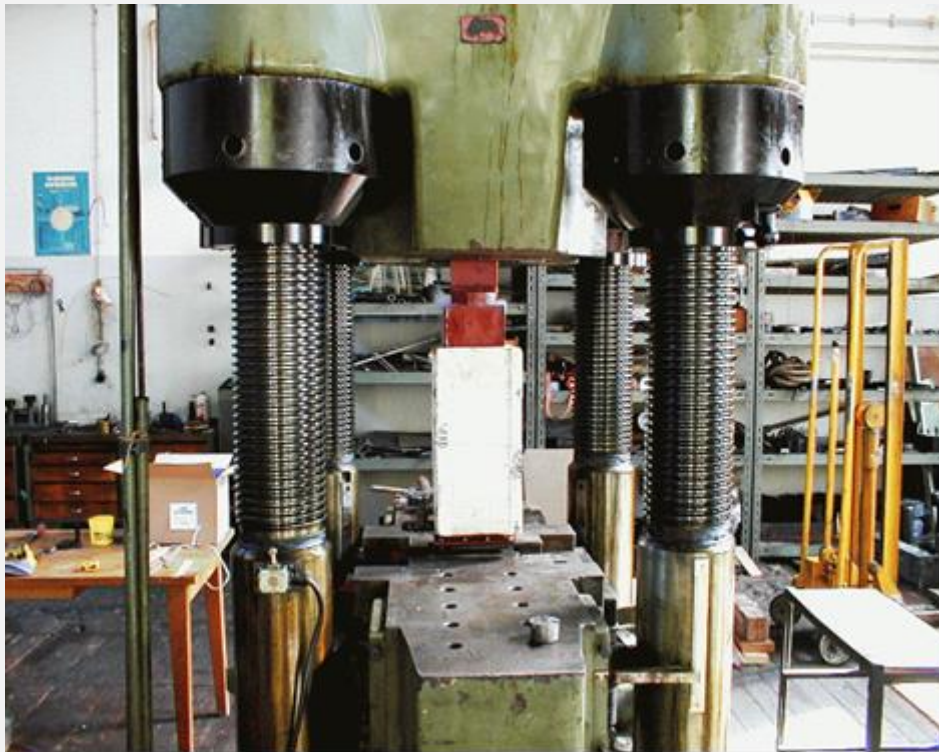


Fig. 8. Insulated tube filled with dry ice

The flow-chart of dynamic (fatigue) testing:

1. Updated increase of static loading until the level of 400 kN with the following decrease on the level 100 kN.
2. Updated increase of static loading on the level 400 kN.
3. Fatigue part of testing with specification of frequency as well as lower and upper amplitude levels of vibrating axial forces and the start of fatigue testing.
4. After obtaining required amplitude level the start of numbering of cycles.

Some numerical and experimental results obtained are summed up in Tables 1 and 2.

Table 1. Some results of static testing

Specimen Nr.	Temperature	Ultimate axial force in kN	
		calculated	tested
4	-60° C	642	640
5	-60° C	628	625
8	-30°	614	610
9	-30° C	639	635

Table 2. Some results of the fatigue testing

Specimen Nr.	Temperature [°C]	Upper & lower load amplitudes [kN]		Upper & lower force amplitudes [kN]		Frequency [Hz]	Number of cycles	
							Calculated	tested
3	25	450	100	400	200	3.7	5276	5300
6	-60	400	200	-	-	2.8	4157	4180
7	-30	400	200	-	-	2.8	2364	2400

3D-plotting of the simulation model which used is shown in Fig. 9. The stress developments at some levels of axial load adopted are given in Figs. 10, 11 and 12.

The comparison of numerical and experimental results submits the surmise about the adaptability of above theoretical approaches for analysis of ultimate fatigue behaviour of slender steel specimens at low temperatures. Besides, theoretical, numerical and experimental results presented provide some image dealing with complicated ultimate behaviour of steel specimens dependent of temperature.

7 CONCLUSIONS

Theoretical, numerical and experimental activities presented were made in scope of expertise for industrial facility ELBA, Kremnica, Slovakia, in order to explain some problems of steel specimens adopted in electric air conductors of high voltage lines being located in northern territories with cool temperatures. The results obtained were immediately adopted in scope of new developments of such conductor lines.

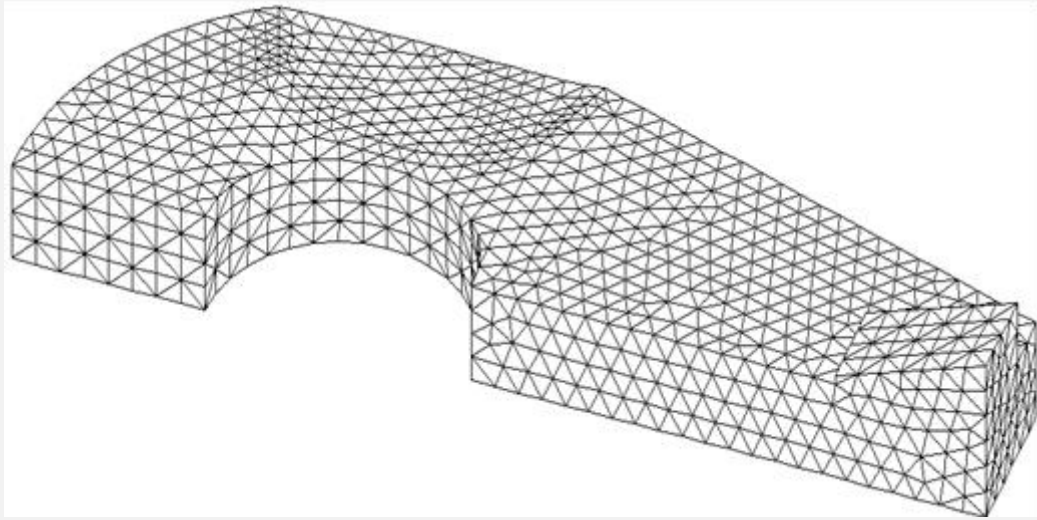


Fig. 9. 3D-model used for calculation (4944 Solid Elements, 1889 Nodes)

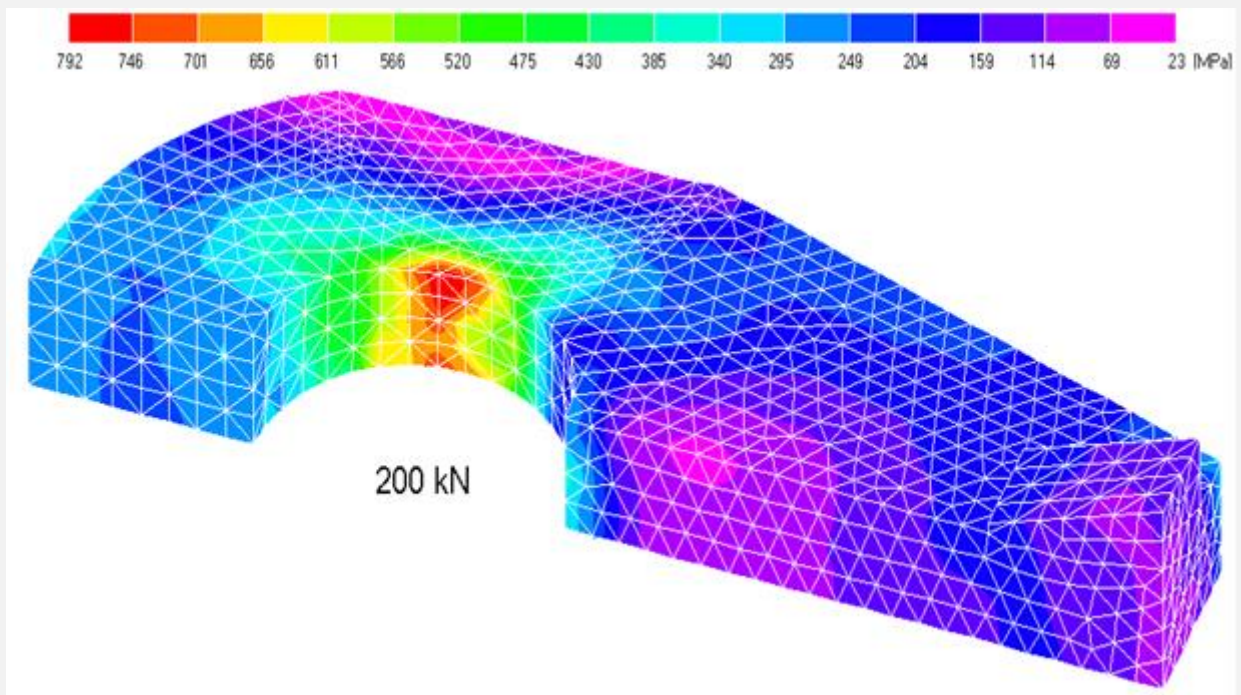


Fig.10. Stress configuration at axial load level 200 kN

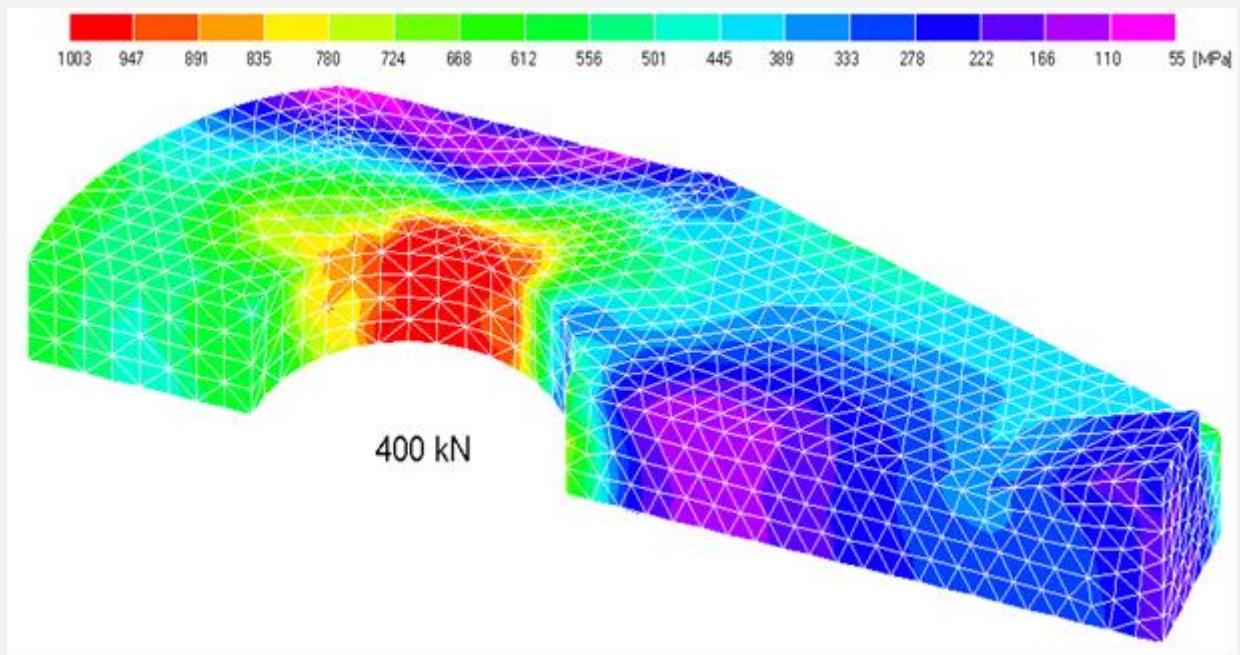


Fig. 11. Stress configuration at axial load level 400 kN

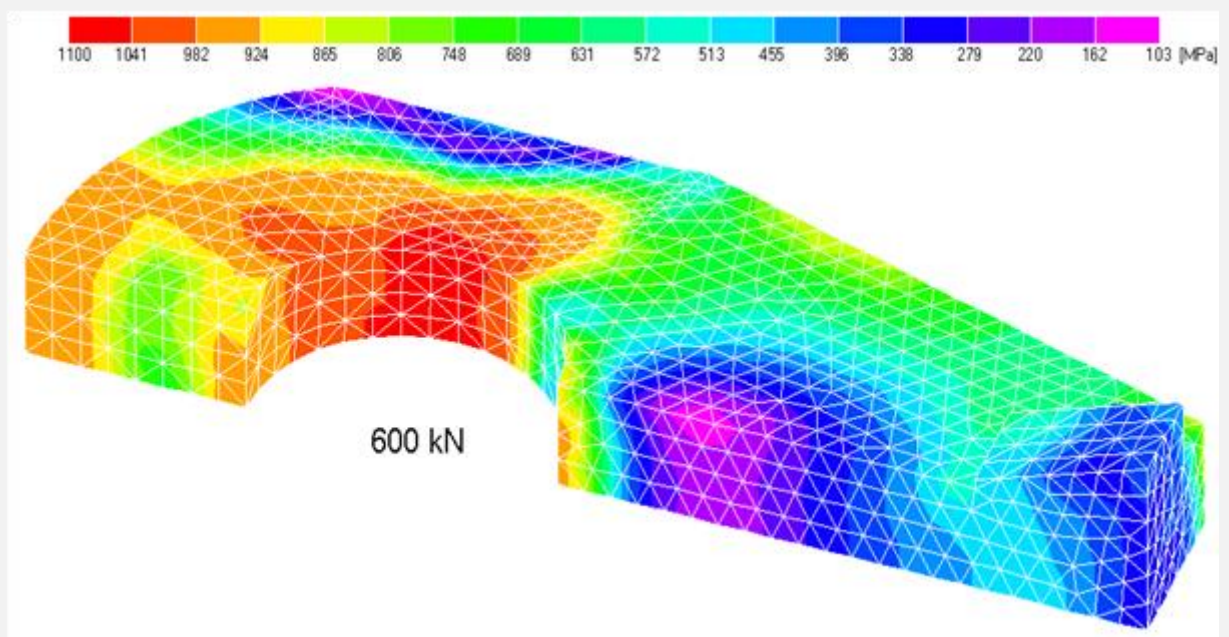


Fig. 12. Stress configuration at axial load level 600 kN

ACKNOWLEDGEMENT

Author is indebted to industrial enterprise ELBA, Kremnica, Slovak Republic, for suggestion and financial support of the research presented.

8 REFERENCES

- [1] Tesar, A.: Transfer Matrix Method, KLUWER Academic Publishers, Dordrecht/Boston/London, 1988.
- [2] Tesar, A. and Svolik, J.: Wave distribution in fibre members subjected to kinematic forcing. Int. Journal for Communication in Numerical Mechanics, 9, 1993
- [3] Simo, J.C.: On a fully three-dimensional finite strain viscoelastic damage model – formulation and computational aspects. Comput. Meth. Engng. 29, 1990
- [4] Huston, R.L. and Passerello, C.E.: Multibody structural dynamics including translation between the bodies. Computers and Structures, 11, 1980
- [5] Adeli, H. And Yeh, C.: Perception Learning in Engineering Design. Microcomputers in Civil Engineering, 4, 1989
- [6] Lu, W. and Mäkeläinen, P.: A neural network model for local and distortional buckling behaviour of cold-formed steel compression members. Proceedings of 9-th Nordic Steel Construction Conference, Helsinki, 2001
- [7] Tesar, A.: Mémoires of Engineer. EDIS, Žilina, 2019
- [8] Budiansky, B.: Micromechanics. Computers and Structures, Vol. 16, Issues 1-4, 1983, pp. 3-12
- [9] Budiansky, B.: Micromechanics II. Proceedings of the 10-th US National Congress of Applied Mechanics, Austin, Texas, 1986, pp. 1-8.
- [10] Tesar, A.: Nonlinear Structural Dynamics. EDIS, Žilina, 2016
- [11] Tesar, A.: Transfer Matrix Method - new developments and applications. Lambert Academic Publishing, 2015

ABSTRACT

FATIGUE OF STEEL SPECIMENS AT LOW TEMPERATURES

Alexander TESAR

Fatigue behaviour of 3-D steel structural specimens at low temperatures was investigated in this paper. Simulation model adopting backpropagation neural network approach is used for the analysis. The updated Lagrange formulation of motion combined with pseudo-force technique in the FETM-wave approach was used for the treatment of non-linear problems. Each step of iteration approaches the solution of linear problem and the feasibility of parallel processing combined with backpropagation neural network is established. Numerical and experimental analysis is submitted in order to demonstrate the efficiency of the procedures suggested.

Key words: fatigue, FETM-wave approach, low temperature, neural network, parallel processing, pseudo-force technique, ultimate behaviour

APSTRAKT

ZAMOR ČELIČNIH UZORAKA PRI NISKIM TEMPERATURAMA

Alexander TESAR

U radu je analizirano ponašanje čeličnih uzoraka pod dejstvom zamornog opterećenja pri niskim temperaturama. Za analizu su primenjene neuronske mreže i pristup propagacija unazada (backpropagation). Nelinearni problem je tretiran pomoću modifikovane Lagranževove formulacije kretanja, kombinovane sa metodom pseudo-sile u FETM pristupu. Svaki korak iteracije se približava rešenju linearnog problema, pri čemu je ilustrovana primenljivost paralelnog procesuiranja u kombinaciji sa neuronskim mrežama. Poređenjem numeričkih i eksperimentalnih rezultata demonstrirana je efikasnost predloženog postupka.

Ključne reči: zamor, FETM pristup, niska temperatura, neuronske mreže, paralelno procesuiranje, metoda pseudo-sile, granično ponašanje